Conclusions

We have shown that relatively large exchange couplings are observed when metal ions bind to the pyridine nitrogen of NITpPy essentially through a $\sigma-\pi$ nonorthogonality mechanism. Further, it is very important that both ferro- and antiferromagnetic couplings can be observed.

These observations have an important consequence for elaborating strategies to design molecules that can offer multiple exchange pathways, potentially capable of allowing the building of three-dimensional magnetic structures. Indeed the nonzero coupling observed when a metal ion is bound to the pyridine nitrogen gives exciting perspectives if the NO groups can be induced to interact with other paramagnetic centers. This has indeed found to be the case with gadolinium(III) ions.[42]

Acknowledgment. The financial support of the CNR, of the Progetto Finalizzato "Materiali Speciali per Tecnologie Avanzate", and of MURST is gratefully acknowledged. Thanks are due also to the Laboratorio di Chimica Applicata of the Università della Calabria, Calabria, Italy.

Supplementary Material Available: Tables SI-SX, listing crystallographic parameters, anisotropic thermal parameters, hydrogen coordinates, bond lengths, bond angles, and least-squares planes for I and II, and Table SXI, reporting the more intense peaks of the X-ray powder diffractograms of II and IV (15 pages); Tables SXII and SXIII, listing observed and calculated structure factors of I and II, respectively (22 pages). Ordering information is given on any current masthead page.

(42) Benelli, C.; Caneschi, A.; Gatteschi, D.; Pardi, L. Work in progress.

Contribution from the Department of Chemistry, University of Florence, Florence, Italy, and Departement de Recherche Fondamentale, Centre d'Etudes Nucleaires, Grenoble, France

Linear-Chain Gadolinium(III) Nitronyl Nitroxide Complexes with Dominant Next-Nearest-Neighbor Magnetic Interactions

Cristiano Benelli,[†] Andrea Caneschi,[†] Dante Gatteschi,*[,†] Luca Pardi,[†] and Paul Rey[‡]

Received February 5, 1990

$Gd(hfac)_3NITiPr$ (hfac = hexafluoroacetylacetonate; NITiPr = 2-isopropyl-4,4,5,5-tetramethyl-4,5-dihyro-1*H*-imidazolyl-1-oxyl 3-oxide) crystallizes in the monoclinic space group $P2_1/n$ with cell parameters a = 11.916 (1) Å, b = 17.625 (9) Å, c = 18.055 (1) Å, β = 96.98 (1)°, V = 3763.82 Å^3, and Z = 4. The structure refinement converged to R = 0.086. The molecular structure of the complex consists of linear chains made up by gadolinium(III) ions bridged by nitronyl nitroxide radicals. The magnetic properties of this compound and of other structurally strictly related lanthanide nitronyl nitroxide complexes are discussed according to a model in which the next-nearest-neighbor interactions are explicitly taken into account. For appropriate values of the exchange parameters the ground state corresponds to a two-spins-up, two-spins-down configuration, which justifies the low effective magnetic moment observed at low temperature.

Introduction

When a spin is under the influence of two neighboring spins that tend to orient it in two opposing ways, the system is said to be magnetically frustrated. The simplest case in which a situation like this occurs is when three spins on a triangle are antiferromagnetically coupled and the preferred spin orientation in the ground state depends on the relative values of the individual coupling constants. Among the practical realizations of this situation, it is worth mentioning the case of Fe_4S_4 ferredoxin,[1] where the understanding of the nature of the frustrated spin triangular arrangement is central to the interpretation of the magnetic properties of the cluster.[2]

The problem of competing interactions in extended magnetic systems has even more far reaching consequences. Spin glasses are, for instance, known to be systems in which competing interactions lead to a spin-frustrated state, and the models that permit the interpretation of the physics of these systems[3,4] have attracted attention even out of the field of magnetic materials. In fact the statistical mechanics that apply to these systems can be usefully applied to develop models for the mechanisms of action of neural networks.[5]

Furthermore, magnetic solids with competing interactions have provided examples of physical systems with fractal dimensionality.[6-8] Helical and conical as well as other exotic magnetic structures have been predicted, and sometimes observed, when competition is present between different magnetic interactions.[9-12]

For their relative simplicity, one-dimensional systems have provided an objective on which to develop and verify theoretical models regarding physical phenomena ranging from collective excitations to transport phenomena and spin dynamics.[13-18] These systems can in principle give rise to competing interactions when the spins are coupled antiferromagnetically to their next-nearest neighbor (nnn) independent of the sign of the interaction with the nearest neighbors (nn). The preferred spin alignment along the chain, however, depends on the relative intensities of the nn and nnn interactions.

Although in the last few years the magnetic properties of several alternating-spin chains have been reported,[19-24] to our knowledge

[†] University of Florence.
[‡] Centre d'Etudes Nucleaires.

(1) Girerd, J. J.; Papaefthymiou, G. C.; Watson, A. D.; Gamp, E.; Hagen, K. S.; Edelstein, N.; Frankel, R. B.; Holm, R. H. *J. Am. Chem. Soc.* **1984**, *106*, 5941.
(2) Papaefthymiou, G. C.; Girerd, J. J.; Moura, I.; Moura, J. J. G.; Munck, E. *J. Am. Chem. Soc.* **1987**, *109*, 4703.
(3) Sherrington, D.; Kirkpatrick, S. *Phys. Rev. Lett.* **1979**, *35*, 1792.
(4) Sherrington, D.; Kirkpatrick, S. *Phys. Rev. B* **1978**, *17*, 983.
(5) Parisi, G. In *Magnetic Properties of Matter*; Borsa, F., Tognetti, V., Eds.; World Scientific Publishing Co. Pte. Ltd.: Singapore, 1988.
(6) von Boehm, J.; Bak, P. *Phys. Rev. Lett.* **1979**, *42*, 122.
(7) Bak, P.; Fukuyama, H. *Phys. Rev. B* **1980**, *21*, 3287.
(8) Mandelbrot, B. B. *The Fractal Geometry of Nature*; W. H. Freeman: New York, 1982.
(9) Harada, I. *J. Phys. Soc. Jpn.* **1984**, *53*, 1643.
(10) Harada, I.; Mikeska, H. J. *Z. Phys. B: Condens. Matter* **1988**, *72*, 391.
(11) Tonegawa, T.; Harada, I. *J. Phys. Soc. Jpn.* **1987**, *56*, 2153.
(12) Rastelli, E.; Tassi, A.; Reatto, L. *Physica C* **1979**, *97B*, 1.
(13) Berlinsky, A. J. In *Highly Conducting One-Dimensional Solids*; Devreese, J. T., Evrad, R. P., Eds.; Plenum Press: New York, 1979; p 1.
(14) Schweitzer, D.; Keller, H. J. In *Organic and Inorganic Low-Dimensional Crystalline Materials*; Delhaes, P.; Drillon, M., Eds.; Plenum Press: New York, 1987; p 219.
(15) Drumheller, J. E. *Magn. Reson. Rev.* **1982**, *7*, 123.
(16) Kokoszka, G. F. In *Low Dimensional Cooperative Phenomena*; Keller, H. J., Ed.; Plenum Press: New York, 1975; p 171.
(17) Richards, P. M. In *Low Dimensional Cooperative Phenomena*; Keller, H. J., Ed.; Plenum Press: New York, 1975; p 147.
(18) Gatteschi, D.; Sessoli, R. *Magn. Reson. Rev.* **1990**, *15*, 1.

0020-1669/90/1329-4223$02.50/0

Table I. Crystallographic Data for $Gd(hfac)_3NITiPr$

formula $GdC_{25}H_{22}F_{18}N_2O_8$	fw 977.68
a = 11.916 (1) Å	space group $P2_1/n$ (No. 14)
b = 17.625 (9) Å	λ = 0.710 69 Å (Mo Kα)
c = 18.055 (1) Å	ρ_{calcd} = 1.725 g cm^{-3}
β = 96.98 (1)°	μ = 18.60 cm^{-1}
V = 3763.82 Å^3	$R(F_o)$ = 0.0861
Z = 4	$R_w(F_o)$ = 0.0854
T = 17 °C	

there are neither experimental nor theoretical reports specifically regarding alternating-spin linear-chain systems with nn and nnn interactions. By alternating-spin systems we mean one-dimensional materials in which different spins, belonging for instance to different metal ions or to metal ions and organic radicals, respectively, alternate regularly in space.

In the course of our investigation of magnetic materials containing exchange-coupled rare earth ions and organic radicals we have synthesized two linear-chain compounds of the formula $Gd(hfac)_3NITR$ (hfac = hexafluoroacetylacetonate; NITR = 2-*R*-4,4,5,5-tetramethyl-4,5-dihydro-1*H*-imidazolyl-1-oxyl 3-oxide; R = isopropyl, ethyl) that are one-dimensional alternating-spin materials. Their magnetic properties do not agree with either ferro- or antiferromagnetic nn interactions.

We suggest that they are indeed examples of one-dimensional materials with dominant nnn interactions, and we present a simple model to interpret their magnetic properties, together with the crystal structure of $Gd(hfac)_3NITiPr$.

Experimental Section

Synthesis. $Gd(hfac)_3\cdot 2H_2O$ was prepared as previously described.[25,26] NITiPr (NITiPr = 2-isopropyl-4,4,5,5-tetramethyl-4,5-dihyro-1*H*-imidazolyl-1-oxyl 3-oxide) radical was prepared according to literature methods[26,27] and satisfactorily analyzed for C, H, and N.

A 1-mmol amount of $Gd(hfac)_3\cdot 2H_2O$ was dissolved in hot heptane, then 1 mmol of NITiPr was added, and the resulting solution was allowed to cool at 4 °C. Orange elongated crystals suitable for an X-ray structure determination were collected after 1 day and satisfactorily analyzed for $Gd(hfac)_3NITiPr$.

$Gd(hfac)_3NITEt$ (NITEt = 2-ethyl-4,4,5,5-tetramethyl-4,5-dihydro-1*H*-imidazolyl-1-oxyl 3-oxide) was synthesized according to a previously reported method.[22]

X-ray Data Collection and Reduction. A crystal of approximate dimension 0.2 × 0.6 × 0.2 mm was mounted on an Enraf-Nonius CAD4 diffractometer equipped with a Mo Kα X-ray tube and a graphite monochromator. Crystal data are reported in Table I. Cell parameters were determined by 25 machine-centered reflections in the $10° < \theta < 13°$ range. Three test reflections for orientation and intensity control were measured every 160 min, showing no decay during the data collection.

Data were corrected for Lorentz and polarization effects but not for absorption.

Structure Solution and Refinement. The systematic absences ($h0l$, $h + l = 2n+1$; $0k0$, $k = 2n + 1$; $h00$, $h = 2n + 1$; $00l$, $l = 2n + 1$) are only compatible with the $P2_1/n$ space group. The metal ion was localized by the conventional heavy-atom method, and the positions of the other non-hydrogen atoms were found by successive Fourier and difference Fourier syntheses.

As already observed in other complexes containing the hfac ligand,[22,28] disorder was present in the CF_3 groups and this was reflected in the poor quality of the X-ray diffraction data. Due to this fact difficulties were encountered in the crytal structure refinement. Several unsuccessful attempts were made to find a model of the disorder within the trifluoromethyl groups. Finally, the CF_3 groups were refined as rigid group with an idealized tetrahedral geometry, with C–F distances of 1.30 Å and F–C–F angles of 109°.

The refinement converged with a conventional R value of 0.086. Hydrogen atoms were included in the last stage of the refinement in idealized calculated positions. The last calculated difference Fourier map showed peaks of intensity less than 1.1 Å^{-2} having no chemical significance. The programs used for crystallographic computation are reported in ref 29.

Physical Measurements. Magnetic susceptibility data in the range 4.2–300 K were measured by using a fully automated Aztec DSM5 susceptometer equipped with a Bruker B-E15 electromagnet operating at 1.35 T. Temperature variation was obtained with an Oxford CF1200S continuous-flow cryostat. The apparatus was calibrated by measuring the susceptibility of $Gd_2(SO_4)_3\cdot 8H_2O$ at different temperatures. Corrections for diamagnetic contributions were evaluated from Pascal's constants.

EPR spectra were recorded on a Varian E9 spectrometer equipped with MODEL E101 and E110 microwave bridges for X-band and Q-band, respectively. The temperature variation was controlled by means of an Oxford ESR9 continuous-flow cryostat.

Single crystals were oriented with an Enraf-Nonius CAD4 diffractometer and mounted on the perspex rod of a goniometer.

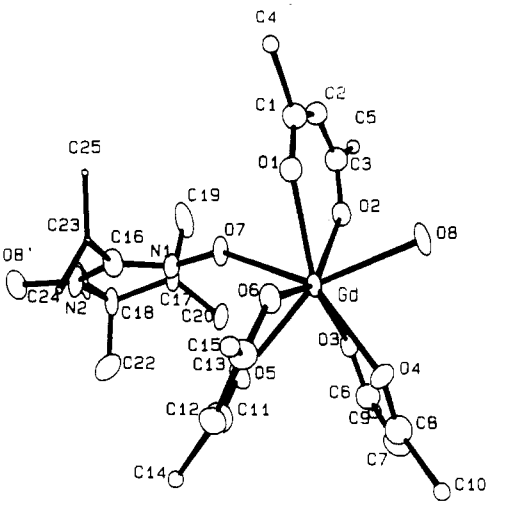

Figure 1. ORTEP drawing of the asymmetric unit of $Gd(hfac)_3NITiPr$. For the sake of clarity fluorine atoms have been omitted and the size of the thermal ellipsoids of the carbon atoms of the isopropyl group have been reduced.

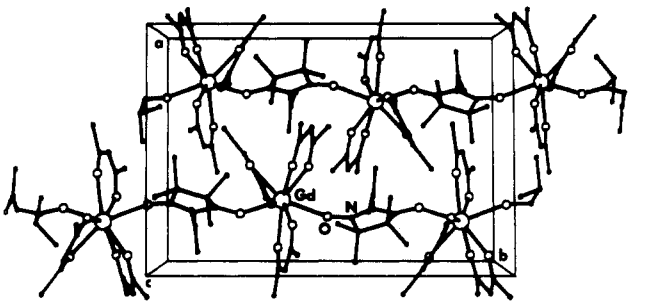

Figure 2. Unit cell representation of $Gd(hfac)_3NITiPr$.

Results

Crystal Structure. The crystal structure of $Gd(hfac)_3NITiPr$ closely resembles that of other rare-earth materials in which nitronyl nitroxide radicals bridge two different trivalent metal ions,

(19) Caneschi, A.; Gatteschi, D.; Laugier, J.; Rey, P. *J. Am. Chem. Soc.* **1987**, *109*, 2191.
(20) Caneschi, A.; Gatteschi, D.; Rey, P.; Sessoli, R. *Inorg. Chem.* **1988**, *27*, 1756.
(21) Caneschi, A.; Gatteschi, D.; Renard, J. P.; Rey, P.; Sessoli, R. *Inorg. Chem.* **1989**, *28*, 2940.
(22) Benelli, C.; Caneschi, A.; Gatteschi, D.; Pardi, L.; Rey, P. *Inorg. Chem.* **1989**, *28*, 275.
(23) Kahn, O.; Pei, Y.; Verdaguer, M.; Renard, J. P.; Sletten, J. *J. Am. Chem. Soc.* **1989**, *110*, 782.
(24) Coronado, E.; Drillon, M.; Fuertes, A.; Beltran, D.; Mosset, A.; Galy, J. *J. Am. Chem. Soc.* **1986**, *108*, 900.
(25) Richardson, M. F.; Wagner, D. F.; Sands, D. E. *J. Inorg. Nucl. Chem.* **1968**, *30*, 1275.
(26) Lamchen, M.; Wittay, T. W. *J. Chem. Soc. C* **1966**, 2300.
(27) Ullman, F. E.; Osieky, J. H.; Boocock, D. G. B.; Darcy, R. *J. Am. Chem. Soc.* **1972**, *94*, 7049.
(28) Benelli, C.; Caneschi, A.; Gatteschi, D.; Pardi, L.; Rey, P. *Inorg. Chem.* **1989**, *28*, 3230.
(29) (a) Sheldrick, G. SHELX 76 System of Computing Programs. University of Cambridge, Cambridge, England, 1976. (b) Johnson, C. K. ORTEP. Report ORNL 3794; Oak Ridge National Laboratory: Oak Ridge, TN, 1965. (c) Rizzoli, C.; Sangermano, V.; Calestani, G.; Andreetti, G. D. CRYSRULER Package. Università degli Studi di Parma, 1986.

Table II. Positional Parameters ($\times 10^4$) and Isotropic Thermal Factors ($Å^2 \times 10^3$) for $Gd(hfac)_3NITiPr$[a]

	x	y	z	U_{eq}/U_{iso}
Gd	2935 (1)	3649 (1)	2628 (1)	67
O1	965 (14)	3511 (9)	3026 (9)	84
O2	1955 (15)	3941 (9)	1592 (9)	88
O3	4339 (14)	3947 (9)	1664 (9)	87
O4	4294 (15)	4378 (10)	3174 (10)	95
O5	4362 (17)	2735 (10)	2716 (10)	108
O6	2755 (15)	3316 (8)	3882 (9)	82
O7	2389 (16)	2484 (8)	2099 (10)	96
O8	2239 (17)	4904 (9)	2851 (11)	111
N1	2648 (19)	1811 (11)	1905 (13)	75
N2	2186 (22)	5586 (11)	3061 (14)	98
C1	132 (14)	3550 (14)	2715 (12)	93 (9)
C2	111 (22)	3736 (15)	1981 (17)	95
C3	970 (23)	3911 (15)	1472 (9)	102 (10)
C4	−1001 (14)	3405 (14)	3269 (12)	216 (21)
C5	805 (23)	4095 (15)	624 (9)	209 (20)
C6	5317 (15)	4144 (15)	1629 (8)	115 (12)
C7	5885 (26)	4480 (18)	2235 (20)	133
C8	5270 (15)	4518 (14)	2947 (11)	115 (12)
C9	5999 (15)	4191 (15)	811 (8)	177 (17)
C10	5921 (15)	4939 (14)	3553 (11)	199 (19)
C11	4802 (15)	2560 (13)	3261 (10)	131 (14)
C12	4457 (24)	2675 (16)	4038 (19)	119
C13	3405 (21)	3072 (14)	4294 (8)	100 (10)
C14	5855 (15)	1997 (13)	3098 (10)	159 (15)
C15	2962 (21)	3124 (14)	5165 (8)	200 (19)
C16	2439 (28)	1195 (17)	2290 (18)	101
C17	3064 (29)	1609 (14)	1113 (18)	91
C18	3427 (30)	782 (14)	1205 (16)	92
C19	2023 (30)	1720 (16)	686 (16)	146
C20	3968 (25)	2164 (14)	786 (18)	125
C21	1973 (33)	5206 (14)	4358 (17)	165
C22	329 (27)	5695 (18)	3695 (22)	164
C23	1868 (35)	1180 (26)	3083 (24)	170
C24	2511 (35)	1037 (22)	3660 (18)	181
C25	779 (33)	1250 (21)	3195 (22)	197
F1	−1872 (14)	3489 (14)	2908 (12)	224 (11)
F2	−990 (14)	2720 (14)	3533 (12)	215 (11)
F3	−1059 (14)	3889 (14)	3816 (12)	238 (12)
F4	1436 (23)	3643 (15)	183 (9)	334 (18)
F5	1094 (23)	794 (15)	473 (9)	261 (13)
F6	249 (23)	3997 (15)	529 (9)	263 (13)
F7	5633 (15)	3670 (15)	391 (8)	245 (12)
F8	7069 (15)	4086 (15)	852 (8)	251 (13)
F9	5850 (15)	4855 (15)	526 (8)	257 (13)
F10	6910 (15)	5158 (14)	3243 (11)	239 (12)
F11	5341 (15)	5526 (14)	3811 (11)	262 (13)
F12	6043 (15)	4475 (14)	4097 (11)	249 (13)
F13	6429 (15)	2170 (13)	2462 (10)	192 (10)
F14	5492 (15)	1303 (13)	3074 (10)	230 (11)
F15	6500 (15)	2059 (13)	3626 (10)	219 (11)
F16	2724 (21)	3826 (14)	5342 (8)	254 (13)
F17	2060 (21)	2711 (14)	5312 (8)	260 (13)
F18	3743 (21)	2880 (14)	5549 (8)	250 (13)

[a] Standard deviations in the last significant digit are in parentheses.

giving rise to a linear-chain molecular framework.[22,29] Positional parameters and selected bond distances and angles are reported in Tables II and III, respectively.

The ORTEP drawing of the asymmetric unit is reported in Figure 1, while the contents of the unit cell are shown in Figure 2. Gadolinium ion has coordination number 8 and a polyhedron of coordination that is best approximated by a dodecahedron. Gd–O distances are in good agreement with those of the other structurally related derivatives of Gd(III) with nitronyl nitroxides and β-diketonates.[22,30,31]

The shortest interchain contacts between metal ions and nitrogen and oxygen atoms of the radicals is 9.02 (3) Å between the gadolinium ion and the N1 atom related by the glide plane, while the shortest Gd–Gd interchain contact is 10.48 Å between the ions related by the inversion center.

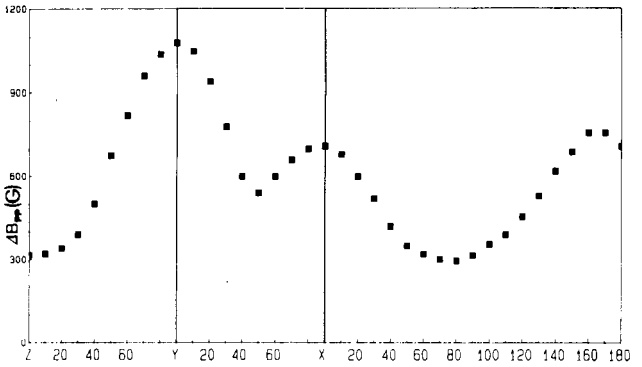

Figure 3. Angular dependence of the line width of the room-temperature X-band EPR spectrum of $Gd(hfac)_3NITEt$.

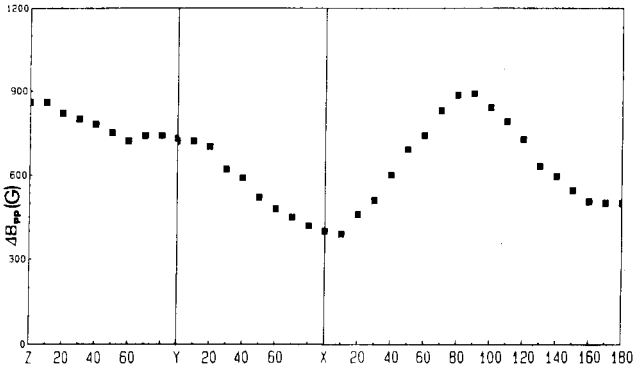

Figure 4. Angular dependence of the line width of the X-band EPR spectrum of $Gd(hfac)_3NITEt$ at 20 K.

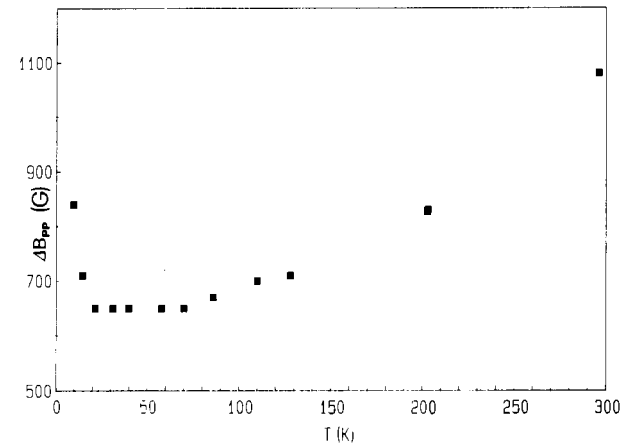

Figure 5. Temperature dependence of the line width of the EPR spectrum of $Gd(hfac)_3NITEt$ when the static magnetic field is parallel to the chain direction (b axis).

EPR and Magnetic Data. A single isotropic signal centered at $g = 2$ is present in the powder spectra of $Gd(hfac)_3NITiPr$ and $Gd(hfac)_3NITEt$ complexes in the temperature range 4.2–300 K. From the liquid-helium temperature value of the line width, ΔB_{pp}, of ca. 1000 G for $Gd(hfac)_3NITEt$ and of ca. 1500 G for $Gd(hfac)_3NITiPr$, ΔB_{pp} decreases to 300 G for the former and to 670 G for the latter derivative at room temperature.

Single crystals suitable for EPR were obtained only for $Gd(hfac)_3NITEt$. For this compound single-crystal EPR spectra were recorded by rotating the crystal around the axis orthogonal to the $(10\bar{1})$ crystal face (x), the b axis (y), and an axis orthogonal to the xy plane. The spectra were recorded at X-band frequency, at room temperature and at 20 K, and at Q-band frequency, at room temperature. For all the crystal orientations and in the investigated temperature range (4.2–300 K) only one signal was detected with isotropic g value of 2.00. The angular dependence of the line width in the X-band spectra at room temperature, shown

(30) Drew, M. G. B. *Coord. Chem. Rev.* **1987**, *24*, 179.
(31) Sinha, S. P. *Struct. Bonding (Berlin)* **1976**, *25*, 69.

Table III. Selected Bond Distances (Å) and Angles (deg) for $Gd(hfac)_3NITiPr$[a]

	Distances		
Gd-O1	2.40 (2)	Gd-O2	2.39 (2)
Gd-O3	2.32(1)	Gd-O4	2.38 (2)
Gd-O5	2.39 (2)	Gd-O6	2.32 (2)
Gd-O7	2.41 (2)	Gd-O8	2.42 (2)
O1-C1	1.22 (2)	O2-C3	1.24 (2)
O3-C6	1.21 (2)	O4-C8	1.21 (2)
O5-C11	1.21 (2)	O6-C13	1.21 (2)
O7-N1	1.24 (2)	O8-N2	1.21 (2)
N1-C16	1.30 (3)	N1-C17	1.48 (4)
C16-C23	1.62 (4)	C17-C18	1.58 (3)
C17-C19	1.59 (4)	C17-C20	1.46 (4)
C23-C24	1.36 (4)	C23-C25	1.30 (4)
	Angles		
O1-Gd-O8	139.8 (6)	O6-Gd-O8	94.4 (5)
O6-Gd-O7	100.4 (5)	O5-Gd-O8	148.9 (6)
O5-Gd-O7	71.3 (6)	O5-Gd-O6	74.7 (6)
O4-Gd-O8	70.6 (6)	O4-Gd-O7	149.5 (6)
O4-Gd-O6	72.7 (6)	O4-Gd-O5	78.3 (6)
O3-Gd-O8	96.8 (6)	O3-Gd-O7	95.8 (6)
O3-Gd-O6	139.3 (6)	O3-Gd-O5	75.7 (6)
O3-Gd-O4	74.5 (5)	O2-Gd-O8	75.2 (6)
O2-Gd-O7	71.9 (6)	O2-Gd-O6	146.3 (6)
O2-Gd-O5	129.0 (6)	O2-Gd-O4	129.8 (6)
O2-Gd-O3	74.3 (6)	O1-Gd-O8	74.6 (6)
O1-Gd-O7	74.3 (6)	O1-Gd-O6	73.3 (6)
O1-Gd-O5	127.0 (6)	O1-Gd-O4	128.4 (6)
O1-Gd-O3	147.4 (6)	O1-Gd-O2	73.1 (6)
Gd-O1-C1	132 (1)	Gd-O2-C3	133 (1)
Gd-O3-C6	133 (1)	Gd-O4-C8	129 (1)
Gd-O5-C11	129 (1)	Gd-O6-C13	133 (1)
Gd-O7-N1	147 (1)	Gd-O8-N2	158 (1)

[a] Standard deviations in the last significant digit are in parentheses.

in Figure 3, has the typical behavior of monodimensional magnetic systems in the high-temperature limit,[17,18] showing, in the z rotation, a maximum along the chain axis b and a minimum at 50° from that direction not far from the magic angle value of 54.7°. The Q-band spectra show the same general behavior as the X-band spectra. In Figure 4 is shown the angular dependence of the line width of the X-band EPR spectra at 20 K.

The temperature dependence of the line width of the EPR spectrum was measured by setting the crystal in such a way that the chain axis was parallel to the magnetic field and is shown in Figure 5. From the liquid-helium temperature value of ca. 1000 G, the line width decreases to a minimum of 650 G at about 20 K and then monotonically increases up to the room-temperature value of 1080 G. No g shift was observed on lowering the temperature.

The χT product in the temperature range 4.2–300 K for $Gd(hfac)_3NITiPr$ is reported in Figure 6. From the room-temperature value of 8.05 emu mol^{-1} K, which corresponds to μ_{eff} = 8.02 μ_B and agrees well with that expected for completely uncorrelated $S = {}^7/_2$ and $S = {}^1/_2$ spins, χT starts to decrease at about 60 K and reaches a value of 4.706 emu mol^{-1} K at 4.6 K. The magnetic behavior of $Gd(hfac)_3NITEt$, previously reported,[22] is similar: the χT value starts to decrease at ca. 120 K and reaches a value of 2.55 emu mol^{-1} K at 6 K.

Discussion

As discussed in the previous paper on $Gd(hfac)_3NITEt$,[22] the decrease of χT on decreasing temperature cannot be reconciled with a normal linear chain with only nearest-neighbor interactions. In fact, if the gadolinium ions and the radicals are uncoupled, the material should follow the Curie law and the χT product should be constant with temperature; if they are coupled either ferro- or antiferromagnetically, then the effective magnetic moment should diverge at low temperature, as observed in ferro- and ferrimagnetic one-dimensional materials.

In the previous paper we took into account two possibilities in order to explain the observed decrease of the effective magnetic moment with temperature: one is that the chain is not regular,

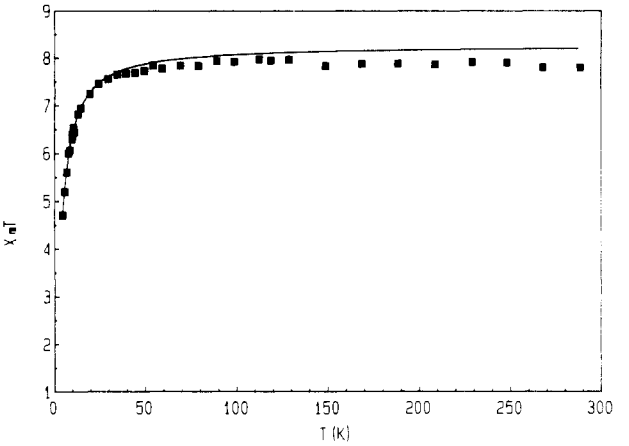

Figure 6. Temperature dependence of the χT product of $Gd(hfac)_3NITiPr$ in the 4.2–300 K temperature range. The line is calculated with the Ising model described in the text.

but the nearest-neighbor exchange interactions are alternating ferro- and antiferromagnetic, and the other is that antiferromagnetic interchain interactions are strong enough to effectively couple the spins. Both models allowed a reasonable fit of the experimental data but only with unreasonably large values of the coupling constants.

The present data definitively rule out the possibility of large interchain interactions because the room-temperature single-crystal EPR spectra unambiguously indicate the magnetic monodimensionality of the $Gd(hfac)_3NITEt$ derivative. In fact the angular dependence of the line width of the EPR spectra for $Gd(hfac)_3NITEt$ has the typical features of the diffusive regime of the spin correlation function, with a maximum along the chain direction and a minimum at the magic angle from that which are the signatures of a one-dimensional magnetic material.[16-18] If significant exchange interactions were active between the chains, then the diffusive effects would be destroyed and the angular dependence of the line width would follow a $(1 + \cos^2 \theta)$ behavior.[15,16] Therefore, we can estimate that the ratio of the inter- to intrachain coupling constant is smaller than ca. 10^{-3} cm^{-1},[20,32] ruling out the possibility that the interchain interactions determine the spin alignment at high temperatures. At low temperature the $(3 \cos^2 \theta - 1)^n$ angular dependence is lost. This is in line with the fact that the enhancement of the secular component, which in fact determines the magic angle behavior of the line width, is brought about by the $q \simeq 0$ modes, which tend to keep all the spins parallel to each other. When the temperature is decreased, unless the coupling within the chain is ferromagnetic, the $q \simeq 0$ modes become progressively less important and the line tends to follow a $(1 + \cos^2 \theta)$ dependence.[15-18]

The temperature dependence of the line width measured with the static magnetic field along the chain direction shown in Figure 4 is also reminiscent of one-dimensional magnetic systems.[15,33]

On the basis of the structural data for $Gd(hfac)_3NITiPr$, which show that the distances between the chains are even larger for this compound, we must conclude that interchain dipolar interactions must even be smaller for this derivative. Thus, the explanation of the magnetic properties must be found within the chains. Since nn interactions are not sufficient to justify them, it is necessary to introduce nnn interactions.

An antiferromagnetic interaction, of the order of 10 cm^{-1}, was found to be operative between the radicals in a linear-chain yttrium (III) nitronyl nitroxide complex that has a structure very similar to that of the gadolinium derivatives described here.[28] It has been suggested that the origin of the coupling is superexchange through the empty 5s and 4d atomic orbitals of the metal ions. The 6s atomic orbital provides a similar superexchange pathway in lan-

(32) Hennessy, M. J.; McElwee, C. D.; Richards, P. M. *Phys. Rev. B: Solid State* **1973**, *7*, 930.
(33) Cheung, T. T. P.; Soos, Z. G.; Dietz, R. E.; Merrit, F. R. *Phys. Rev. B.* **1978**, *17*, 1266.

thanide–radical complexes. In fact an antiferromagnetic coupling between nitronyl nitroxide radicals has been observed in Eu(hfac)$_3$NITR and Eu(hfac)$_3$(NITR)$_2$ complexes,[22,34] which can be rationalized only by the intervening mediation of the metal ion. We can therefore reasonably assume that an antiferromagnetic coupling of the same order of magnitude between the radicals is active in Gd(hfac)$_3$NITR complexes.

In discrete gadolinium nitronyl nitroxide complexes, where two radicals coordinate to the metal ion in a pseudo trans fashion, the magnetic properties could be interpreted only by introducing a weak antiferromagnetic coupling between the radicals.[35] On the other hand, the nn gadolinium–radical interaction was found to be ferromagnetic and of the order of 1–2 cm^{-1}, therefore, the interaction between the radicals should be dominant in all these systems. In this hypothesis the radical spins would preferentially orient antiparallel to each other, while the gadolinium spins would be under the influence of two contrasting nn interactions and would become frustrated. The spin-frustration condition would result in a low-temperature limit of the χT product equal to that of the uncorrelated $S = {}^7/_2$ spins, i.e. 7.877 emu mol^{-1} K, or $\mu_{eff} = 7.9$ μ_B, well above the observed low-temperature value. The only way to obtain a magnetic model that at least qualitatively reproduces the observed behavior is to turn on also a weak antiferromagnetic interaction between the gadolinium(III) ions. In this hypothesis it is easy to visualize a state in which two neighboring spins along the chain are up and the next two are down, giving an overall antiferromagnetic ground state at 0 K. In fact, in this situation a given spin conforms to the requirements of the two next-nearest neighbors and to that of one nearest neighbor, opposing only to one nn interaction. Therefore, this model should be possible if both the nnn interactions are relatively strong.

The problem of competing interactions in one-dimensional magnetic structures has been thoroughly investigated in the physical literature where it has been shown that linear chains of classical spins with nn and nnn antiferromagnetic coupling give helimagnetic order at 0 K.[10] Studies on one-dimensional spin $S = {}^1/_2$ Heisenberg magnetic systems with nn and nnn competing interactions have been performed within a transfer-matrix approach and have provided the variation of thermodynamic properties as a function of the ratio of the competing coupling constants.[9]

A model for the phase diagram of the rare-earth magnet CeSb has been developed within an Ising approximation framework, introducing ferromagnetic nn interactions and nnn antiferromagnetic interaction between the magnetic ions in the lattice.[6] The phase stable at low temperature is that corresponding to the ground state described as "two spins up, two spins down", while when the temperature is increased, the system goes through an infinity of commensurate phases described by more complex spin states, a phenomenon which is known as the "Devil's staircase".[6] The same spin configuration is theoretically predicted at 0 K in a one-dimensional lattice of spins $S = {}^1/_2$, with first and second nearest-neighbor magnetic interactions, treated within the Ising model by using the Bethe approximation.[35]

Both helimagnetic[36] and two-spins-up, two-spins-down ground states can explain the observed magnetism of Gd(hfac)$_3$NITR complexes. The rather complicated mathematics involved in the development of a Heisenberg exchange chain model led us to choose the Ising model in order to test the validity of our qualitative predictions. The approximation seems to be quite strong for a system built up by magnetically isotropic gadolinium(III) ions and organic radicals. The justification we offer is that the Ising model is simple and allows quantitative predictions.

The Hamiltonian of the system is written as

$$H = J_{Gd\text{-}R}\sum_{nn} S_{Gd}{}^z S_R{}^z + J_{R\text{-}R}\sum_{nnn} S_R{}^z S_R{}^z + J_{Gd\text{-}Gd}\sum_{nnn} S_{Gd}{}^z S_{Gd}{}^z - g\mu_B B_z \sum (S_R{}^z + S_{Gd}{}^z) \quad (1)$$

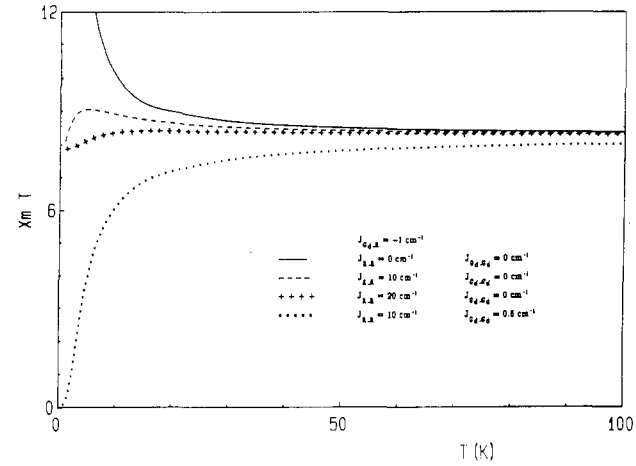

Figure 7. Calculated values of the χT product for a linear chain of alternating $S = {}^7/_2$ and $S = {}^1/_2$ spins with nn and nnn magnetic interactions (see text).

where $J_{Gd\text{-}R}$ is the nn coupling constant between gadolinium ion and radical, $J_{Gd\text{-}Gd}$ and $J_{R\text{-}R}$ are the nnn coupling constants, and $S_i{}^z$ are the spin angular momentum components of the i species along the quantization axis z. Isotopic $\mathbf{g} = 2$ tensors are taken on the two magnetic centers.

Generalizing the statistical model of Kramers and Wannier,[37] we consider a finite linear chain of alternating $S = {}^7/_2$ and $S = {}^1/_2$ spins as that depicted in the following scheme:

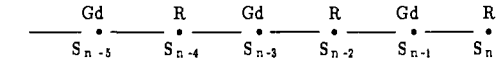

The probability $P(S_n)$ of the radical spin that terminates the linear chain being either in the $M_s = {}^1/_2$ or in the $M_s = {}^{-1}/_2$ spin state is expressed in terms of the same probability for the radical spin S_{n-4}. In the limit of an infinite chain this probability is

$$\lambda P(S_n) = \sum P(S_{n-4}) \exp[K(S_nS_{n-1} + S_{n-1}S_{n-2} + S_{n-2}S_{n-3} + S_{n-3}S_{n-4}) + K'(S_nS_{n-2} + S_{n-2}S_{n-4}) + K''(S_{n-1}S_{n-3} + S_{n-3}S_{n-5}) + C(S_n + S_{n-1} + S_{n-2} + S_{n-4})] \quad (2)$$

where $K = J_{Gd\text{-}R}/kT$, $K' = J_{R\text{-}R}/kT$, $K'' = J_{Gd\text{-}Gd}/kT$, and $C = g\mu_B B/kT$, the sum runs over S_{n-1}, S_{n-3}, $S_{n-5} = \pm{}^7/_2, \pm{}^5/_2, \pm{}^3/_2, \pm{}^1/_2$ and S_{n-2}, $S_{n-4} = \pm{}^1/_2$, and λ is an appropriate proportionality constant. Relation 2 has the form of an eigenvalue problem. The solution of this problem gives the two eigenvalues λ_1 and λ_2. When the length of the chain tends to infinity, the smaller eigenvalue is negligible and the partition function of the system takes the form $Z = \lambda^N$, where λ is the largest eigenvalue. By means of the partition function all the thermodynamic quantities of the system can be expressed. The magnetization M, for instance, is given by[37]

$$M = (g\mu_B N)\frac{1}{\lambda}\frac{\delta Z}{\delta \lambda} \quad (3)$$

where λ and C have the same meanings as above and the magnetic susceptibility of the system can be calculated, in the limit $kT \gg g\mu_B B$, as $\chi = M/B$.

Sample calculations were performed by varying the relative values of the J constants, and the results are shown in Figure 7. When $J_{R\text{-}R}$ and $J_{Gd\text{-}Gd}$ are set equal to zero and $J_{Gd\text{-}R} < 0$, the χT curve diverges, as expected for a ferromagnetic chain (full line in Figure 7). If $J_{R\text{-}R}$ is taken as positive (antiferromagnetic nnn coupling), then the χT curve initially increases, passes through a maximum, and then converges to 7.877 emu mol^{-1} K, the value for isolated gadolinium(III) ions (dashed lines in Figure 7). If also $J_{Gd\text{-}Gd}$ is taken as positive, then χT decreases monotonically and tends to zero at low temperature (dotted lines in Figure 7). These results are in line with the qualitative predictions worked out above. In particular it is rewarding that the dotted lines have

(34) Benelli, C.; Caneschi, A.; Gatteschi, D.; Pardi, L.; Rey, P.; Shum, D. P.; Carlin, R. L. *Inorg. Chem.* **1989**, *28*, 272.
(35) Obokata, T.; Oguchi, T. *J. Phys. Soc. Jpn.* **1968**, *25*, 322.
(36) De Raedt, H.; De Raedt, B. *Phys. Rev. B.* **1979**, *19*, 2595.
(37) Kramers, H. A.; Wannier, G. H. *Phys. Rev.* **1941**, *60*, 252.

the same general behavior as experimentally observed for Gd(hfac)$_3$NITR.

The results of the calculations for $J_{Gd-R} > 0$ are similar to that described above, with a diverging behavior in the ferrimagnetic regime ($J_{R-R} = 0$ and $J_{Gd-Gd} = 0$), a frustrated behavior when $J_{R-R} > 0$ and $J_{Gd-Gd} = 0$, and a monotonically decreasing behavior when a weak antiferromagnetic coupling between gadolinium ions is turned on.

Starting from the encouraging conclusions of the sample calculations, we attempted a quantitative fit of the magnetic data for Gd(hfac)$_3$NITEt and Gd(hfac)$_3$NITiPr that yielded $J_{Gd-R} = -0.41$ cm^{-1}, $J_{R-R} = 5.08$ cm^{-1}, and $J_{Gd-Gd} = 0.98$ cm^{-1} for the former and $J_{Gd-R} = -0.42$ cm^{-1}, $J_{R-R} = 5.32$ cm^{-1}, and $J_{Gd-Gd} = 0.38$ cm^{-1} for the latter. In the limit imposed by the intrinsic inadequacy of the Ising model for interpreting the data of a system made up by highly isotropic species, these results can be considered satisfactory. In fact the J_{Gd-R} and J_{R-R} values compare well with those previously reported for other mononuclear gadolinium-radical complexes.[34] The J_{Gd-Gd} constants are fairly large for interactions between rare-earth ions, but comparable values have been recently observed from inelastic neutron-scattering measurements in rare-earth pairs.[38] The fact that a nnn coupling constant, namely J_{Gd-Gd} in Gd(hfac)$_3$NITEt, is larger than the nn coupling constant could be at first sight surprising; it must however be taken into account that the comparison should be made between the constants scaled by a factor $1/n_1n_2$, where n_1 and n_2 are the number of electron on the first and on the second interacting centers, respectively; moreover, we are in this case comparing coupling constants that derive from different exchange mechanisms. Further, it must be recalled that the two NO groups of the radical are equivalent; therefore, a superexchange interaction is effectively transmitted to the two ends of the nitronyl nitroxide. The difference between the J_{Gd-Gd} constants obtained in the two cases can be tentatively attributed to the different intrachain Gd-Gd distances in the two derivatives. Actually for Gd(hfac)$_3$NITEt two different Gd-Gd distances are observed namely 8.59 and 8.64 Å, while in Gd(hfac)$_3$NITiPr the Gd-Gd intrachain distance is 8.88 Å.

(38) Doenni, A.; Furrer, A.; Blank, H.; Heidemann, A.; Gudel, H. U. *J. Phys.* **1988**, *49*, C8-1513.

Conclusions

The Gd(hfac)$_3$NITR (R = ethyl, isopropyl) compounds represent unique one-dimensional magnetic materials in which nnn interactions determine the preferred spin orientation at low temperature. Within the simple Ising model that we worked out quantitatively, the ground state corresponds to a two-spins-up, two-spins-down configuration, but it cannot be excluded that within a more correct Heisenberg exchange approach the ground state is characterized by a more complicated spin arrangement.[10] Presumably, neutron diffraction studies could provide a definitive answer to this problem. The rapid increase of the EPR line width below 20 K may be in fact indicative of peculiar spin dynamics associated with the ground state.

It is very important to notice how the magnetic interactions between rare-earth ions and organic radicals give rise to unexpected behaviors, which are due to the fact that the interactions between metal ions and radicals are relatively weak, while the superexchange between radicals through the metal ions (and between metal ions through the radicals) is relatively strong.

Acknowledgment. Thanks are expressed to MURST, to the CNR, and to the Progetto Finalizzato "Materiali Speciali per Tecnologie Avanzate" for financing the research.

Supplementary Material Available: Listings of crystallographic and experimental data (Table SI), complete bond distances and angles (Table SII), and anisotropic thermal parameters (Table SIII) (6 pages); a table of observed and calculated structure factors (Table SIV) (13 pages). Ordering information is given on any current masthead page.

Contribution from the Department of Chemistry, University of Florence, Florence, Italy, and Departement de Recherche Fondamentale, Centre d'Etudes Nucleaires, Grenoble, France

Structure and Magnetic Properties of Manganese(II) Carboxylate Chains with Nitronyl Nitroxides and Their Reduced Amidino-Oxide Derivatives. From Random-Exchange One-Dimensional to Two-Dimensional Magnetic Materials

Andrea Caneschi,[1a] Dante Gatteschi,*[1a] Maria Chiara Melandri,[1a] Paul Rey,[1b] and Roberta Sessoli[1a]

Received February 20, 1990

Two compounds of formula Mn(pfpr)$_2$(NITMe) (I) and [Mn(pfpr)$_2$]$_2$(NITMe)(IMHMe) (II), respectively, where pfpr = pentafluoropropionate, NITMe = 2,4,4,5,5-pentamethyl-4,5-dihydro-1*H*-imidazolyl-1-oxyl 3-oxide, and IMHMe = 2,4,4,5,5-pentamethyl-4,5-dihydroimidazole 3-oxide, have been synthesized. The latter crystallizes in the monoclinic $P2_1/c$ space group with $a = 13.898$ (3) Å, $b = 19.089$ (4) Å, $c = 7.867$ (3) Å, $\beta = 94.90$ (2)°, $R = 0.052$, and $Z = 4$. The structure consists of manganese carboxylate chains that have as additional bridging ligands NITMe and IMHMe molecules randomly distributed along the chains. Hydrogen bonds between neighboring pairs of NITMe and IMHMe molecules connect the chains in puckered planes perpendicular to *a*. The magnetic properties of [Mn(pfpr)$_2$]$_2$(NITMe)(IMHMe) are consistent with a random-exchange one-dimensional model, while those of Mn(pfpr)$_2$(NITMe) indicate a two-dimensional system with antiferromagnetic interactions between ferrimagnetic chains. The magnetic properties suggest that the crystal structure of I is similar to that of II with the hydrogen bonds replaced by longer contacts between noncoordinated NO groups of the radicals.

Introduction

The so-called metal-radical approach has been successfully employed in the synthesis of molecular based ferromagnets.[2] It consists in the use of stable organic radicals such as the nitronyl nitroxides, 2-R-4,4,5,5-tetramethyl-4,5-dihydro-1*H*-imidazolyl-1-oxyl 3-oxide, NITR, as ligands for transition-metal ions, which can thus be connected in infinite structures. The individual metal-radical coupling can be either ferro- or antiferromagnetic, and in this way one-dimensional ferro- and ferrimagnets were obtained.[2-5] In a few cases these were found to undergo a phase

(1) (a) University of Florence. (b) Centre d'Etudes Nucleaires.
(2) Caneschi, A.; Gatteshi, D.; Sessoli, R.; Rey, P. *Acc. Chem. Res.* **1989**, *22*, 392.
(3) Caneschi, A.; Gatteschi, D.; Laugier, J.; Rey, P. *J. Am. Chem. Soc.* **1987**, *109*, 2191.
(4) Caneschi, A.; Gatteschi, D.; Rey, P.; Sessoli, R. *Inorg. Chem.* **1988**, *27*, 1756.
(5) Caneschi, A.; Gatteschi, D.; Renard, J.-P.; Rey, P.; Sessoli, R. *Inorg. Chem.* **1989**, *28*, 2940.

0020-1669/90/1329-4228$02.50/0